Charge ordering and elastic anomalies in $Pr_{0.65}Ca_{0.35}MnO_3$

2002 J. Phys.: Condens. Matter 14 3973

(http://iopscience.iop.org/0953-8984/14/15/311)

INSTITUTE OF PHYSICS PUBLISHING JOURNAL OF PHYSICS: CONDENSED MATTER

J. Phys.: Condens. Matter **14** (2002) 3973–3979 PII: S0953-8984(02)31882-4

Charge ordering and elastic anomalies in $Pr_{0.65}Ca_{0.35}MnO_3$

S Seiro[1,2], H R Salva[1], M Saint-Paul[2], A A Ghilarducci[1], P Lejay[2], P Monceau[2], M Nunez-Regueiro[2] and A Sulpice[2]

[1] Centro Atomico Bariloche, Av. E Bustillo km 9, 5, 8400 Bariloche, Argentina
[2] Centre de Recherche sur les Très Basses Temperatures (CNRS), 25 av. des Martyrs, BP 166, 38042 Grenoble Cedex 9, France

Received 13 December 2001
Published 4 April 2002
Online at stacks.iop.org/JPhysCM/14/3973

Abstract

Ultrasonic sound velocity and attenuation at 15 MHz, the Young modulus at 5 kHz and the shear modulus at 1 Hz were measured for polycrystalline $Pr_{0.65}Ca_{0.35}MnO_3$ in the temperature range 100–300 K. Upon cooling from room temperature a common behaviour can be observed for the different moduli: a small softening above the charge-ordering temperature $T_{CO} \sim 230$ K, followed by a large hardening below T_{CO}. A corresponding attenuation peak is observed at T_{CO} in ultrasound measurements. The modulus effect is related to a strain–order parameter coupling proportional to Q^2, where Q is the order parameter. The critical exponent β estimated from the elastic constant behaviour is much smaller than the mean-field one.

1. Introduction

Mixed-valence manganese oxides have been thoroughly studied because of their colossal magnetoresistance (CMR), indicating that they have potential application in magnetic devices, as well as because of the variety of phenomena that they exhibit resulting from the interplay of different interactions: superexchange and double-exchange mechanisms, Coulomb interaction and the Jahn–Teller effect.

The properties of the manganese perovskites $A_{1-x}B_xMnO_3$, where A is a trivalent rare-earth cation and B a divalent alkali, can be varied by changing the doping x [1], and the relative and average sizes of A and B [2,3]. Replacing a proportion x of A with lower-valence B cations induces the same proportion of Mn^{3+} ions to adopt a 4+ valence. This allows the e_g electron in Mn^{3+} to migrate to unoccupied levels in Mn^{4+}, depending on the Mn–O–Mn angle and the relative orientation of the t_{2g} localized spins in the Mn sites involved.

In compounds such as $Pr_{1-x}Ca_xMnO_3$, where the ionic radii of A and B cations are relatively small, buckling of oxygen octahedra around Mn ions is produced in order to compensate for the free space. A further distortion of the $Mn^{3+}O_6$ octahedra is provided by the Jahn–Teller

effect of Mn^{3+} ions, which causes a splitting of e_g orbitals by stretching or compressing specific Mn^{3+}–O bond lengths. In $Pr_{1-x}Ca_xMnO_3$ the distortion with respect to the ideal cubic perovskite is orthorhombic [1]. This structural distortion implies a deviation of Mn–O–Mn angles from 180°, decreasing the rate of hopping of the e_g electrons from Mn^{3+} to Mn^{4+} sites. As a consequence of this, $Pr_{1-x}Ca_xMnO_3$ compounds present an insulating electrical behaviour for all x. Poor electron transfer weakens the double-exchange ferromagnetic interaction. As ferromagnetic interactions are weak, superexchange dominates, and (Pr, Ca) manganites present an antiferromagnetic state over a wide doping range ($0.3 < x < 0.95$) [4]. Below a certain temperature T_{CO}, a superstructure appears, corresponding to ordering of Mn^{3+} and Mn^{4+} on alternate lattice sites. Simultaneously with the charge ordering, orbital ordering takes place and a structural deformation develops below T_{CO}, which saturates near T_N. Recent studies of $Pr_{0.5}Ca_{0.5}MnO_3$ show that the ordering is not commensurate with a wavevector $q = (1/2 - \varepsilon, 0, 0)$, where ε takes a finite value below T_{CO} and decreases—until it reaches saturation—to a small non-zero value below T_N [5], as has also been reported for $La_{0.5}Ca_{0.5}MnO_3$ [6].

Ultrasonic measurements of the sound velocity and attenuation near structural phase transitions can probe the order parameter and give information on the dynamical properties. In the case of CMR manganites, ultrasonic methods have been successfully applied in the study of $La_{1-x}Ca_xMnO_3$ [7]. In the present work the focus is on the study of the charge-ordering transition in $Pr_{0.65}Ca_{0.35}MnO_3$.

2. Experimental details

The ceramic sample was prepared by thoroughly mixing powders of Pr_6O_{11}, $SrCO_3$, CaO and MnO_2 in stoichiometric proportions, and pressing it into a rod under 1 kbar. Samples of different sizes were cut from the bar and annealed at 1300 °C for five days in oxygen. Sample No 1 (a cylinder of $\phi \sim 3$ mm and $L \sim 6$ mm) was used for resistivity, magnetization, AC susceptibility and ultrasonic measurements, sample No 2 (a $1 \times 1 \times 5$ mm^3 parallelepiped) for Hz elastic measurements and sample No 3 (a $0.5 \times 1.4 \times 5$ mm^3 parallelepiped) for kHz elastic measurements.

Resistivity measurements at zero field were performed in a standard four-wire configuration. Magnetization measurements were performed in a SQUID magnetometer at a field of 100 Oe, and AC susceptibility measurements in a home-made susceptometer at 5 kHz.

Shear modulus measurements were performed on a forced inverted torsion pendulum at a frequency of 1 Hz and a temperature rate of 0.5 K min^{-1}. The angular deformation was less than 1×10^{-5}. Medium-frequency (5 kHz) Young modulus data were obtained in a conventional vibrating-reed spectrometer at a temperature rate of 0.5 K min^{-1}. For high-frequency (ultrasound) data the standard pulse-echo technique was used at 15 MHz with $LiNbO_3$ transducers. The longitudinal sound velocity variation was measured by phase-coherent detection. Attenuation data were obtained by a Matec 2470 attenuation recorder. The temperature rate was approximately 1.5 K min^{-1}.

3. Results

The absolute sound velocity at room temperature was found to be 6000 m s^{-1} for the longitudinal mode (v_L) and 2800 m s^{-1} for the transverse mode (v_T). The measured sample density (ρ) was 90% of the ideal one. From the absolute sound velocity and density, values for different elastic moduli at room temperature could be estimated. The bulk modulus

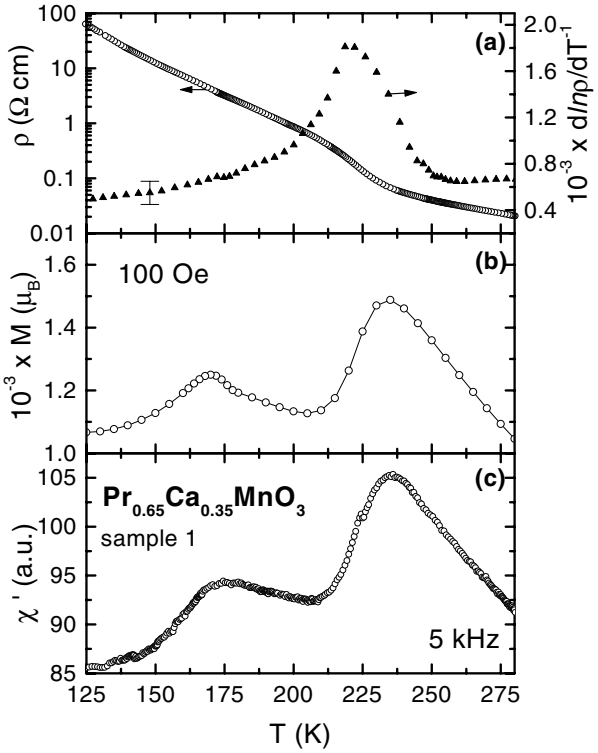

Figure 1. (*a*) Resistivity ρ (open circles) and $\partial \ln \rho / \partial T^{-1}$ (full triangles), (*b*) magnetization at 100 Oe and (*c*) AC susceptibility at 5 kHz for $Pr_{0.65}Ca_{0.35}MnO_3$ (sample No 1) as a function of temperature. The transition to the charge-ordered state occurs at T_{CO} ∼230 K and antiferromagnetic order sets in at $T_N \sim 170$ K.

$B = \rho(v_L^2 - 4/3v_T^2)$ obtained in this manner is 135 GPa, the shear modulus $G = \rho v_T^2$ is 44 GPa and the Young modulus $E = G(3 - 4v_T^2/v_L^2)/(1 - v_T^2/v_L^2)$ is 120 GPa. The Poisson ratio $\sigma(1 - 2v_T^2/v_L^2)/(2 - v_T^2/v_L^2)$ was estimated to be 0.36.

The temperature dependence of the resistivity is shown in figure 1(*a*). An insulating behaviour is observed throughout the measured temperature range. At the charge-ordering temperature, $T_{CO} \sim 230$ K, there is an increase of resistivity. This reflects the ordered localization of e_g electrons in the charge-ordered phase. The logarithmic derivative of the resistivity exhibits a significant peak at the transition. No effects are observed at the magnetic ordering temperature.

In figure 1(*b*) we show the magnetization as a function of temperature. A significant peak is observed at $T_{CO} \sim 230$ K, coincident with the transition to the charge-ordered state, and another peak at lower temperature indicates antiferromagnetic ordering. The peak at T_{CO} indicates a change in the nature of the magnetic interaction, which is ferromagnetic above T_{CO} (the extrapolation of m^{-1} versus T reaches zero at a positive Curie temperature). But ferromagnetism is destroyed with the ordering of carriers below T_{CO}, where superexchange becomes predominant and the Mn spins order antiferromagnetically at ∼170 K.

The behaviour of the real component χ' of the AC susceptibility at 5 kHz (figure 1(*c*)) is similar to that observed for magnetization. A susceptibility peak is observed at T_{CO}, and at lower temperatures another peak appears coincident with T_N.

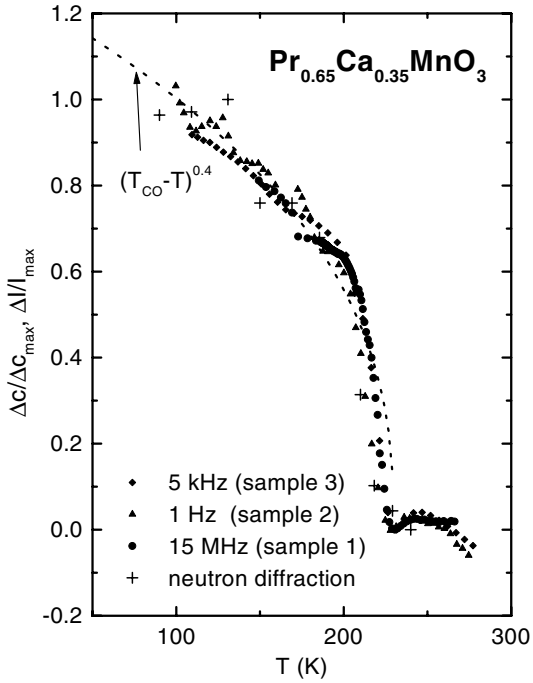

Figure 2. Comparison of the behaviours as a function of temperature of the different moduli (the shear modulus at 1 Hz measured for sample No 2 and represented by upward-pointing triangles, the Young modulus at 5 kHz measured for sample No 3 and represented by diamonds, and the longitudinal modulus at 15 MHz measured for sample No 1 and represented by circles), with the $(3, 1/2, 2)$ superlattice intensity as taken from Yanagisawa *et al* [8]. The normalization factors were: 0.25 at 1 Hz, 0.38 at 5 kHz, 0.15 at 15 MHz and 1100 counts for neutron intensity data. The dotted curve represents a $(T_{CO} - T)^{0.4}$ behaviour.

In figure 2 elastic measurements at different frequencies are shown. The data have been normalized by the corresponding modulus change at 100 K with respect to the value at T_{CO}. Upward-pointing triangles represent 1 Hz shear modulus data measured for sample 2, and $\Delta G/G$ (100 K) is 0.25. Diamonds represent the 5 kHz Young modulus measured for sample 3, and the normalization factor $\Delta E/E$ (100 K) has been taken as 0.38. The high-frequency (15 MHz) longitudinal modulus change measured for sample 1 is represented by circles, and $\Delta c/c(100\,\mathrm{K}) = 0.15$. The data shown were taken on cooling. In general, the different moduli present a common behaviour: upon cooling, there is first a softening above T_{CO}, then the modulus reaches a minimum at T_{CO}, and below T_{CO} a considerable hardening as a function of temperature is observed. A similar behaviour is exhibited by normalized data for the $(3, 1/2, 2)$ superlattice reflection intensity, taken from Yanagisawa *et al* [8], represented in figure 2 by crosses and normalized by dividing by 1100 counts. The dotted line represents a $(T_{CO} - T)^{\mu}$ behaviour, with $\mu = 0.4$.

At 15 MHz a well defined attenuation peak appears at the CO transition, as can be seen in figure 3. This peak should be associated with the scattering of the sound wave due to order parameter fluctuation over time, originating from the coupling between the order parameter and the strain. The attenuation peak is shifted to lower temperature with respect to the modulus minimum at 1.5 K.

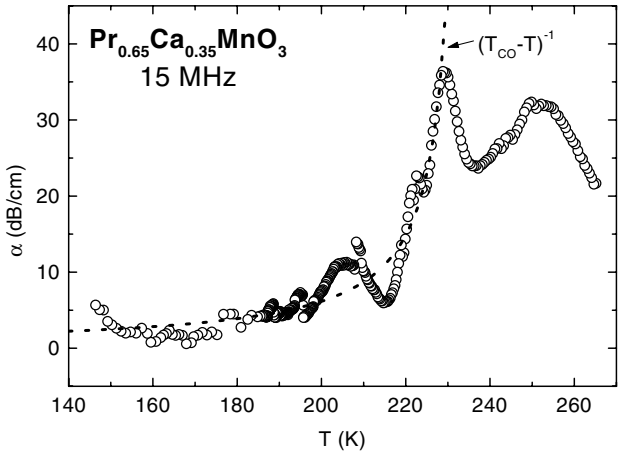

Figure 3. Attenuation at 15 MHz as a function of temperature. An attenuation peak is observed associated with the CO transition, but its maximum is shifted to 1.5 K below T_{CO}. The dotted curve represents a $(T_{CO} - T)^{-1}$ behaviour.

4. Discussion

The effects observed at T_{CO} for the different measured properties provide clear evidence of the interplay that exists among the various degrees of freedom. The ordering of e_g electrons in definite lattice sites decreases the electrical conductivity, and this in turn affects the magnetic interactions among the localized spins, since the reduced mobility of carriers entails a decrease of double-exchange ferromagnetism in favour of superexchange. This is reflected eventually in the onset of an antiferromagnetic state below T_N. But a significant anomaly is observed also in different elastic moduli around T_{CO}, indicating that the lattice degrees of freedom are also affected by the ordering. Further evidence of this is provided by Jirák *et al* [5], who observed for $x = 0.5$ a pseudotetragonal distortion of the lattice parameters below T_{CO}, stabilizing at T_N, and an incommensurate modulation of wavevector $(1/2 - \varepsilon, 0, 0)$, where ε depends on the temperature.

As a first approximation, the energy F of the system near the CO transition may be written as $F(Q, e) = F_L(Q) + F_E(e) + F_I(Q, e)$, where Q is the order parameter and e is the mean strain. F_L represents the Landau energy:

$$F_L(Q) = \tfrac{1}{2}aQ^2 + \tfrac{1}{4}bQ^4,$$

and $F_E(e)$ stands for the elastic energy:

$$F_E(e) = \tfrac{1}{2}c_0e^2,$$

where c_o is a background elastic constant taken at $Q = 0$. $F_I(Q, e)$ is an interaction energy of the form

$$F_I(Q, e) = heQ^2 + le^2Q^2,$$

where terms linear in Q have been left out since the transition is of a non-ferrodistortive type (there is a doubling of the unit cell at the transition, as reported by Yanagisawa *et al* [8]) and in this case strain can only couple with even powers of the ordering quantity [9]. The stress σ on the sample can be obtained as $\sigma = \partial F/\partial e$ and the corresponding elastic modulus as $c = \partial\sigma/\partial e$. For temperatures below T_{CO} the change in modulus may be written as

$$c - c_0 = -2h^2/b + 2I\langle Q\rangle^2,$$

where $\langle Q \rangle$ represents the static value of the order parameter. The first term is a softening of the elastic constant at the transition, while the second term, due to biquadratic coupling of the strain and order parameter, gives the strong hardening below the transition, thus reproducing the experimental behaviour of the elastic moduli shown in figure 2.

Further evidence that biquadratic coupling is responsible for the anomalous hardening below T_{CO} is furnished by the fact that the elastic moduli have the same temperature dependence as the neutron superlattice intensity I. The latter behaves as $I = I_o(T_{CO} - T)^{2\beta}$ in the vicinity of a critical transition, β being the critical exponent of the order parameter. A rough estimate of 0.2 for β has been obtained (see the dotted curve in figure 2) but it should be taken into account that this is merely an average value, due to the inhomogeneity of the ceramic. However, this value is far from $\beta = 0.5$ predicted by mean-field theory, indicating that fluctuations should be important in this system. This is also supported by the presence of an attenuation peak at the transition, as can be observed in figure 3.

Treating the behaviour near the transition as a relaxation process [9], for $\omega\tau \ll 1$, the attenuation can be expressed as

$$\alpha = \Delta c\, \omega^2 \tau / 2dV^3,$$

where ω is the frequency of measure, τ the characteristic relaxation time associated with order parameter fluctuations, d the density and V the sound velocity. Thus, if $\Delta c \sim (T_{CO} - T)^{-\mu}$, $\alpha \sim (T_{CO} - T)^{-\rho}$ and $\tau \sim (T_{CO} - T)^{-z\nu}$, the product of the static (z) and dynamic (ν) critical exponents of the relaxation time can be obtained:

$$z\nu = \mu + \rho.$$

The attenuation behaves approximately as if $\rho \sim 1$, as can be seen in figure 3. In this way the estimate $z\nu \sim 1.4$ can be obtained. This value is higher than the one calculated within mean-field theory, which suggests significant fluctuations in the system. As already mentioned, the attenuation peak is not coincident with the minimum in the elastic constant, but shifted towards lower temperatures. This peak occurs when the characteristic time of the measurement, ω^{-1}, equals the relaxation time of the system. So, if $\tau = \tau_o t^{-z\nu}$, an estimate of τ_o can be obtained: $\tau_o \sim 10^{-13}$ s.

5. Conclusions

To summarize, elastic modulus measurements were performed at 1 Hz (shear modulus), 5 kHz (Young modulus) and 15 MHz (longitudinal modulus) for different samples of $Pr_{0.65}Ca_{0.35}MnO_3$. A minimum was found at $T_{CO} \sim 230$ K in all moduli, together with an attenuation peak in the case of ultrasound measurements. A substantial hardening of the modulus is observed below T_{CO}. This effect is associated with the coupling of charge/orbital and lattice degrees of freedom. The behaviour of the modulus can be reproduced by introducing a coupling between the strain induced by the ultrasonic wave and the order parameter, consisting of two terms: a term in eQ^2 responsible for the softening at the transition, and a term in e^2Q^2 reproducing the hardening below T_{CO}. A rough estimate of the critical exponent $\beta \sim 0.2$ was obtained from elastic measurements, and its value was found to be much smaller than the mean-field-theory prediction. This, together with the occurrence of an attenuation peak and the rather high estimated value obtained for $z\nu$, could indicate that fluctuations play an important role in systems of this kind. However, for a more reliable estimation of the critical coefficients and a more detailed analysis of the coupling energy, single-crystalline samples should be investigated.

References

[1] Jirák Z, Krupiéka S, Šimša Z, Dlouhá M and Vratislav S 1985 *J. Magn. Magn. Mater.* **53** 153
[2] Hwang H Y, Cheong S W, Radaelli P G, Marezio M and Batlogg B 1995 *Phys. Rev. Lett.* **75** 914
[3] Sánchez R D, Salva H R, Caneiro A, Niebieskikwiat D and Monceau P 1999 *J. Physique* IV **9** 333
[4] Martin C, Maignan A, Hervieu M and Raveau B 1999 *Phys. Rev.* B **60** 12 191
[5] Jirák Z, Damay F, Hervieu M, Martin C, Raveau B, André G and Bourée F 2000 *Phys. Rev.* B **61** 1181
[6] Radaelli P G, Cox D E, Marezio M and Cheong S W 1997 *Phys. Rev.* B **55** 3015
[7] See for example:
Ramirez A P, Cheong S W and Schiffer P 1997 *J. Appl. Phys.* **81** 5337
Zheng R K, Zhu C F, Xie J Q and Li X G 2000 *Phys. Rev.* B **63** 024427
[8] Yanagisawa O, Izumi M, Hu W Z, Huang K H, Nakanishi K and Nojima H 1999 *Physica* B **271** 235
[9] Lüthi B and Rehwald W 1981 *Structural Phase Transitions I (Springer Topics in Current Physics vol 23)* ed K A Müller and H Thomas (Berlin: Springer)